A first-in-class inhibitor of parasite FtsH disrupts plastid biogenesis in human pathogens

Katherine Amberg-Johnson[1,3], Suresh M. Ganesan[4], Hernan A. Lorenzi[5], Jacquin C. Niles[4], Ellen Yeh[1,2,3,*]

[1]Department of Biochemistry, [2]Pathology, and [3]Microbiology and Immunology, Stanford Medical School
[4]Department of Biological Engineering, Massachusetts Institute of Technology
[5]Department of Infectious Disease, The J. Craig Venter Institute
*Corresponding author

There is an urgent need for antimalarials with distinct mechanisms-of-action to combat resistance to frontline drugs. The malaria parasite *Plasmodium falciparum* and related apicomplexan pathogens contain an essential, non-photosynthetic plastid organelle, the apicoplast[1,2], which is a key antiparasitic target. Despite its biomedical potential, broadly effective antimalarials targeting the apicoplast have been elusive due to the slow onset-of-action of drugs that inhibit apicoplast translation[3,4] and the apicoplast's limited metabolic function in the symptomatic stage of *Plasmodium*[5]. Apicoplast biogenesis depends on novel, but largely cryptic, mechanisms for protein/lipid import and organelle inheritance during parasite replication[6,7]. These critical pathways present untapped opportunities to discover new parasite-specific drug targets. We used an innovative chemical rescue screen[5] to identify the natural product antibiotic, actinonin[8], as a first-in-class antimalarial compound inhibiting apicoplast biogenesis. Both chemical-genetic interaction and resistant mutation indicated that the unexpected target of actinonin in *P. falciparum* and *Toxoplasma gondii* is FtsH1, a homolog of a bacterial membrane AAA metalloprotease. We show that *Pf*FtsH1 is essential for apicoplast biogenesis and parasite replication, making it the first apicomplexan-specific regulator of organelle biogenesis to be identified in a forward screen. Taken together, our findings demonstrate that FtsH1 is a novel and, importantly, druggable antimalarial target. Development of actinonin derivatives as FtsH1 inhibitors will have significant advantages over existing apicoplast-targeting compounds with improved drug kinetics, lower potential for clinical resistance, and multistage efficacy against multiple human parasites.

Because our molecular understanding of apicoplast biogenesis is limited, we performed a chemical screen to identify compounds that disrupt apicoplast biogenesis. Out of >400 antimalarial compounds tested (Extended Data Table 1)[9,10], we identified a single natural product antibiotic, actinonin[8], as a novel inhibitor of apicoplast biogenesis. Previously we demonstrated that biosynthesis of the isoprenoid precursor, isopentenyl pyrophosphate (IPP), is the sole essential function of the apicoplast in blood-stage *P. falciparum*[5]. As such, compounds that target the apicoplast cause parasite growth inhibition that is fully rescued by the addition of IPP in the growth media. Actinonin caused *P. falciparum* growth inhibition in a single replication cycle (EC_{50} = 3.2 μM; 95% CI 2.49-4.13) that was rescued by IPP (EC_{50} = 60.7 μM; 95% CI 49.6-74.5), demonstrating that it

specifically inhibits the apicoplast with clinically-relevant kinetics (Fig. 1a; Extended Data Fig. 1a; Extended Data Table 1). In contrast, current drugs that inhibit translation in the apicoplast cause a characteristic "delayed death" after two replication cycles *in vitro* that limits their antimalarial efficacy and clinical use[3]. When we assessed parasite growth inhibition and apicoplast defects caused by one of these known apicoplast drugs, chloramphenicol, (Extended Data Fig. 1b and 2a,c) actinonin clearly had more rapid antimalarial activity.

Furthermore, actinonin-treated *P. falciparum*, rescued for growth with IPP, no longer replicated their apicoplast and produced daughter parasites lacking apicoplasts, consistent with a defect in apicoplast biogenesis[5] (Fig. 1b-c, Extended Data Fig. 2a,e). Again, this inhibition phenotype contrasts with that of inhibitors known to disrupt MEP isoprenoid precursor biosynthesis in the apicoplast[5,9,11]. When we assessed the inhibition phenotype of fosmidomycin, a MEP inhibitor that is in clinical trials for antimalarial treatment, it also showed single-cycle antimalarial activity rescued by IPP (Extended Data Fig. 1b). Notably, though, fosmidomycin did not cause apicoplast loss (Extended Data Fig 2a,d). Taken together, actinonin's inhibition phenotype distinguishes it from known inhibitors that disrupt apicoplast translation and metabolism (Extended Data Fig 1b and 2) and indicates that it has a novel mechanism-of-action.

To further elucidate its mechanism-of-action, we first took a candidate-based approach to identify its target. Actinonin potently inhibits the bacterial and mitochondrial peptide deformylase (PDF), an enzyme that co-translationally removes the formyl group from the initiator methionine[12]. Because the apicoplast translation machinery is prokaryotic in origin and contains a PDF, we tested whether the apicoplast PDF is the target of actinonin[13]. In mitochondria, translation inhibitors suppress the effects of actinonin since translation is upstream of PDF activity[14]. Surprisingly, apicoplast translation inhibition did not suppress the effects of actinonin (Extended Data Fig. 3), suggesting apicoplast PDF is not the target of actinonin.

We next took an unbiased approach to identify the target of actinonin by attempting to isolate actinonin-resistant *P. falciparum* but were unsuccessful using multiple selection methods, including chemical mutagenesis of the starting population. Instead we turned to *Toxoplasma gondii*, a related apicomplexan parasite, because it is easier to grow to large numbers and to genetically modify. As in *P. falciparum*, actinonin treatment caused growth inhibition (EC_{50}= 13.7 μM; 95% CI 13.2-14.2; Extended Data Fig 4) and apicoplast loss[15] (Fig. 2a) in *T. gondii*, suggesting a similar mechanism-of-action. We selected for actinonin-resistant *T.gondii* and determined the whole-genome sequences for eight independently selected clones (Fig. 2b). Five of these clones harbored a N805S mutation in the metalloprotease domain of the membrane AAA protease *TgFtsH1* (TGGT1_ 259260) (Fig. 2d; Extended Data Table 2). *Tg*FtsH1 was compelling for two reasons. First, *Tg*FtsH1 localizes to the apicoplast[16]. Second, actinonin is a peptide mimetic containing a metal-binding hydroxamic acid, a class of molecules that typically binds metalloproteases[12,17]. Confirming this resistance mutation, replacement of the endogenous *TgFtsH1(WT)* locus with the allele encoding *TgFtsH1(N805S)* was sufficient to confer actinonin resistance in *T. gondii* (Fig. 2c). The increased actinonin EC_{50} in this

mutant was similar to that measured for the actinonin-resistant clones that arose following drug selection. Taken together, the known metalloprotease binding of actinonin, the predicted metalloprotease activity of TgFtsH1, and the validated actinonin-resistant mutation in *TgFtsH1* support FtsH1 as the target of actinonin in *T. gondii*, providing a strong candidate for validation in *P. falciparum*.

The *P. falciparum* genome contains three FtsH homologs (Pf3D7_1119600, Pf3D7_1239700, and Pf3D7_1464900). One of these, *Pf*FtsH1 (Pf3D7_1239700) is most closely related to *Tg*FtsH1 by phylogenetic analysis[18]. Unlike *Tg*FtsH1, *Pf*FtsH1 was previously reported to localize to the mitochondria, not the apicoplast[18]. However the same study reported that *Pf*FtsH1 undergoes internal cleavage, such that the localization of the *N*-terminal fragment containing the ATPase and protease domains was unclear. Setting aside its ambiguous localization, we sought to determine whether *Pf*FtsH1 is required for apicoplast biogenesis and the relevant target of actinonin. We constructed a *P. falciparum* strain in which the endogenous *PfFtsH1* locus was modified with a *C*-terminal FLAG epitope and 3' UTR tetR-DOZI-binding aptamer sequences to regulate its expression[19]. As expected, *Pf*FtsH1 expression was downregulated when the tetR-DOZI repressor bound the aptamer sequences, and restored when anhydrotetracycline, which disrupts this interaction, was added (Fig. 3a, Extended Data 5).

To test whether *Pf*FtsH1 is essential for apicoplast biogenesis, we downregulated *Pf*FtsH1 and observed a nearly 4-fold decrease in parasitemia after 3 replication cycles, compared to parasites expressing normal levels of *Pf*FtsH1 (Fig 3b, Extended Data Fig. 6a). This growth defect observed after multiple replication cycles is weaker than the single-cycle growth inhibition observed upon actinonin treatment and likely reflects partial knockdown, which has been reported using this tet-regulation system (personal communication, Dan Goldberg). Significantly, growth of *Pf*FtsH1 knockdown parasites was restored by addition of IPP, indicating *Pf*FtsH1 is essential specifically for an apicoplast function (Fig 3b, Extended Data 6a). Finally, we confirmed that loss of *Pf*FtsH1 led to apicoplast loss. Using qPCR for genes in the apicoplast and nuclear genome, we observed a steady decrease in the apicoplast:nuclear genome ratio upon knockdown of *Pf*FtsH1 and growth rescue with IPP compared to control parasites, consistent with loss of the apicoplast[5] (Fig. 3c). These results demonstrate that *Pf*FtsH1 is essential and required for apicoplast biogenesis, making it the first protein with a novel function in apicoplast biogenesis identified in an unbiased screen.

Finally, because knockdown of *Pf*FtsH1 phenocopies the apicoplast biogenesis defect of actinonin, we determined whether knockdown of *Pf*FtsH1 sensitized parasites to actinonin. Indeed, when *Pf*FtsH1 expression was downregulated, the actinonin EC_{50} decreased >50-fold compared to control parasites (Fig. 3d). Since these growth inhibition assays were performed over a single replication cycle, the downregulation of *Pf*FtsH1 did not significantly affect parasite growth, and the actinonin EC_{50} could be measured without confounding growth inhibition caused by the decrease in *Pf*FtsH1 levels (Fig. 3b, Extended Data Fig. 6b). Importantly, PfFtsH1 downregulation did not change the EC_{50} of fosmidomycin, indicating that the hypersensitivity to actinonin after PfFtsH1 downregulation is not due to general apicoplast disruption or parasite death (Extended

Data Fig. 6c). Combined with the target identification in *T. gondii*, this chemical-genetic interaction strongly implicates FtsH1 as the target of actinonin in apicomplexan parasites.

Our study represents a rare example of a forward screen to uncover cryptic cellular pathways in *Plasmodium*[20,21]. Acquired by secondary endosymbiosis of an alga, the apicoplast is evolutionarily distinct. Apicomplexan FtsH1's role in organelle biogenesis is not conserved in homologs found in mitochondria or primary chloroplasts[22] and likely represents a novel pathway unique to secondary endosymbionts in this parasite lineage[7,15,23,24]. Based on the critical function of FtsH homologs in membrane protein quality control and complex assembly[22], we propose that FtsH1 regulates the proteolysis of key apicoplast membrane protein(s) during parasite replication. FtsH1 offers a rare foothold into a novel apicoplast biogenesis pathway that will yield deeper insight into the molecular mechanisms of eukaryogenesis and uncover additional antiparasitic targets.

Most importantly, our findings present an exciting opportunity for antimalarial drug discovery. FtsH1 inhibitors will have significant advantages over existing antimalarials that target apicoplast metabolism or translation. While metabolic needs vary throughout the parasite lifecycle and even between the same stage of different *Plasmodium* species[25,26], apicoplast biogenesis is required at every proliferative stage of the parasite lifecycle and highly conserved among apicomplexan parasites. For example, apicoplast translation inhibitors which cause delayed biogenesis defects have broad clinical application as malaria prophylaxis targeting liver-stage *Plasmodium* spp and as a partner drug, in combination with faster-acting compounds, for acute parasitic diseases targeting blood-stage *Plasmodium* spp, *Toxoplasma gondii*, and *Babesia* spp. In fact, the utility of these antibiotics as antiparasitics would be greater if not for their slow activity. Inhibition of FtsH1 retains all the benefits of targeting apicoplast biogenesis with no delay in the onset-of-action. Moreover, our inability to select actinonin-resistant *Plasmodium* contrasts with the ready selection of *in vitro* resistance against antibiotics[27] and MEP inhibitors[9,28,29] and indicates a lower likelihood of clinical resistance to FtsH1 inhibitors. Finally, several clinical lead candidates based on the actinonin scaffold have advanced into human clinical trials as bacterial PDF inhibitors[30]. We are currently developing an FtsH1-based assay to facilitate high-throughput screening of actinonin derivatives with increased potency and improved drug properties as antimalarials. Overall, FtsH1 inhibitors have potential for rapid onset, minimal clinical resistance, and multi-stage efficacy against multiple parasitic infections, and routes to identifying a clinical lead candidate are readily accessible.

References

1. McFadden, G. I., Reith, M. E., Munholland, J. & Lang-Unnasch, N. Plastid in human parasites. *Nature* **381,** 482 (1996).
2. Köhler, S. *et al.* A plastid of probable green algal origin in Apicomplexan parasites. *Science* **275,** 1485–1489 (1997).
3. Geary, T. G. & Jensen, J. B. Effects of antibiotics on Plasmodium falciparum in vitro. *Am. J. Trop. Med. Hyg.* **32,** 221–225 (1983).

4. Fichera, M. E. & Roos, D. S. A plastid organelle as a drug target in apicomplexan parasites. *Nature* **390,** 407–409 (1997).
5. Yeh, E. & DeRisi, J. L. Chemical Rescue of Malaria Parasites Lacking an Apicoplast Defines Organelle Function in Blood-Stage Plasmodium falciparum. *PLoS Biol* **9,** e1001138 (2011).
6. Waller, R. F. *et al.* Nuclear-encoded proteins target to the plastid in Toxoplasma gondii and Plasmodium falciparum. *Proc. Natl. Acad. Sci.* **95,** 12352–12357 (1998).
7. Vaishnava, S. & Striepen, B. The cell biology of secondary endosymbiosis--how parasites build, divide and segregate the apicoplast. *Mol. Microbiol.* **61,** 1380–1387 (2006).
8. Gordon, J. J., Kelly, B. K. & Miller, G. A. Actinonin: an antibiotic substance produced by an actinomycete. *Nature* **195,** 701–702 (1962).
9. Wu, W. *et al.* A chemical rescue screen identifies a Plasmodium falciparum apicoplast inhibitor targeting MEP isoprenoid precursor biosynthesis. *Antimicrob. Agents Chemother.* AAC.03342-14 (2014). doi:10.1128/AAC.03342-14
10. Goodman, C. D. & McFadden, G. I. Ycf93 (Orf105), a small apicoplast-encoded membrane protein in the relict plastid of the malaria parasite Plasmodium falciparum that is conserved in Apicomplexa. *PloS One* **9,** e91178 (2014).
11. Jomaa, H. *et al.* Inhibitors of the nonmevalonate pathway of isoprenoid biosynthesis as antimalarial drugs. *Science* **285,** 1573–1576 (1999).
12. Chen, D. Z. *et al.* Actinonin, a naturally occurring antibacterial agent, is a potent deformylase inhibitor. *Biochemistry (Mosc.)* **39,** 1256–1262 (2000).
13. Bracchi-Ricard, V. *et al.* Characterization of an eukaryotic peptide deformylase from Plasmodium falciparum. *Arch. Biochem. Biophys.* **396,** 162–170 (2001).
14. Richter, U. *et al.* A Mitochondrial Ribosomal and RNA Decay Pathway Blocks Cell Proliferation. *Curr. Biol.* **23,** 535–541 (2013).
15. van Dooren, G. G. *et al.* A novel dynamin-related protein has been recruited for apicoplast fission in Toxoplasma gondii. *Curr. Biol. CB* **19,** 267–276 (2009).
16. Karnataki, A., Derocher, A. E., Coppens, I., Feagin, J. E. & Parsons, M. A membrane protease is targeted to the relict plastid of toxoplasma via an internal signal sequence. *Traffic Cph. Den.* **8,** 1543–1553 (2007).
17. Ganji, R. J. *et al.* Structural basis for the inhibition of M1 family aminopeptidases by the natural product actinonin: Crystal structure in complex with E. coli aminopeptidase N. *Protein Sci. Publ. Protein Soc.* **24,** 823–831 (2015).
18. Tanveer, A. *et al.* An FtsH protease is recruited to the mitochondrion of Plasmodium falciparum. *PloS One* **8,** e74408 (2013).
19. Ganesan, S. M., Falla, A., Goldfless, S. J., Nasamu, A. S. & Niles, J. C. Synthetic RNA-protein modules integrated with native translation mechanisms to control gene expression in malaria parasites. *Nat. Commun.* **7,** 10727 (2016).
20. Arastu-Kapur, S. *et al.* Identification of proteases that regulate erythrocyte rupture by the malaria parasite Plasmodium falciparum. *Nat. Chem. Biol.* **4,** 203–213 (2008).
21. Hovlid, M. L. & Winzeler, E. A. Phenotypic Screens in Antimalarial Drug Discovery. *Trends Parasitol.* **32,** 697–707 (2016).

22. Janska, H., Kwasniak, M. & Szczepanowska, J. Protein quality control in organelles — AAA/FtsH story. *Biochim. Biophys. Acta BBA - Mol. Cell Res.* **1833,** 381–387 (2013).
23. Moore, R. B. *et al.* A photosynthetic alveolate closely related to apicomplexan parasites. *Nature* **451,** 959–963 (2008).
24. Spork, S. *et al.* An Unusual ERAD-Like Complex Is Targeted to the Apicoplast of Plasmodium falciparum. *Eukaryot. Cell* **8,** 1134–1145 (2009).
25. Srivastava, A. *et al.* Stage-Specific Changes in Plasmodium Metabolism Required for Differentiation and Adaptation to Different Host and Vector Environments. *PLoS Pathog.* **12,** e1006094 (2016).
26. Shears, M. J., Botté, C. Y. & McFadden, G. I. Fatty acid metabolism in the Plasmodium apicoplast: Drugs, doubts and knockouts. *Mol. Biochem. Parasitol.* **199,** 34–50 (2015).
27. Sidhu, A. B. S. *et al.* In vitro efficacy, resistance selection, and structural modeling studies implicate the malarial parasite apicoplast as the target of azithromycin. *J. Biol. Chem.* **282,** 2494–2504 (2007).
28. Dharia, N. V. *et al.* Use of high-density tiling microarrays to identify mutations globally and elucidate mechanisms of drug resistance in Plasmodium falciparum. *Genome Biol.* **10,** R21 (2009).
29. Guggisberg, A. M. *et al.* A sugar phosphatase regulates the methylerythritol phosphate (MEP) pathway in malaria parasites. *Nat. Commun.* **5,** 4467 (2014).
30. Sangshetti, J. N., Khan, F. A. K. & Shinde, D. B. Peptide deformylase: a new target in antibacterial, antimalarial and anticancer drug discovery. *Curr. Med. Chem.* **22,** 214–236 (2015).

Methods

Chemicals

Fosmidomycin was purchased from Santa Cruz Biotechnology and 10mM aliquots were prepared in water. Chloramphenicol was purchased from Sigma Aldrich and 50mM aliquots were prepared in 100% ethanol. Actinonin was purchased from Sigma Aldrich and 25mM aliquots were prepared in 100% ethanol. Anhydrotetracycline was purchased from Sigma and 2.5mM aliquots prepared in 100% ethanol and used at a final concentration of 0.5uM.

Enoxacin, ciprofloxacin, levofloxacin, norfloxacin, novobiocin, coumeramycin, mericitabine, 2'deoxy-2-F-cytidine, gemcitabine, ADEP1a, beta-lactone 4, beta-lactone 7, and rifampin were acquired and solubilized as noted in Supplementary Table 1.

Isopentenyl pyrophosphate (IPP) was purchased from Isoprenoids LC and stored at 2 mg/mL in 70% methanol, 30% 10mM ammonium hydroxide at -80C. To prevent methanol toxicity, aliquots of IPP were dried in the speed vacuum centrifuge before adding to cultures. All drugs were stored at -20C and resuspended just prior to use.

Plasmodium falciparum culture and transfections

P. falciparum D10 (MRA-201), and D10 ACP_L-GFP (MRA-568) were obtained from MR4. *P. falciparum* $NF54^{attB}$ was a gift from David Fidock (Columbia University). NF54

^{attB} strain constitutively expressing Cas9 and T7 Polymerase, generated previously[31], was used in this study. Parasites were maintained in human erythrocytes (2% hematocrit) in RPMI 1640 media supplemented with 0.25% Albumax II (GIBCO Life Technologies), 2 g/L sodium bicarbonate, 0.1 mM hypoxanthine, 25 mM HEPES (pH 7.4), 50 μg/L gentamycin, and 0.4% glucose at 37°C, 5% O_2, and 5% CO_2.

Parasites were transfected using methods already published[21]. Briefly, we used 50 ug of plasmid per 200 uL packed red blood cells (RBCs) adjusted to 50% hematocrit. We used a Bio-Rad Gene Pulser II to preload uninfected RBCs using eight square-wave pulses of 365 V for 1 ms, separated by 100 ms. Preloaded RBCs were resealed for 1 hour at 37C and washed twice in RPMI to remove lysed cells. Schizont stage parasites at 0.5% parasitemia were then allowed to invade half of the preloaded RBCs during two sequential reinvasions. Media was changed daily for the first 12 days and every other day thereafter. Parasites were split 1:1 into fresh blood every 4 days until parasites were visible by Giemsa smear. To select for integration of the pFtsH1 into *P. falciparum* NF54$^{attB\text{-}pPfCRISPR}$ parasites, transfected parasites were maintained in media containing 5 nM WR99210 and 0.5 uM anhydrotetracycline (Sigma) and then selected with 2.5 mg/l Blasticidin S (Sigma) beginning 4 days after transfection.

Toxoplasma gondii culture and transfection

T. gondii RH and *T. gondii* RH Δ*ku80*Δ*hxgprt* strains were a gift from Matthew Bogyo (Stanford University) and maintained by passage through confluent monolayers of human foreskin fibroblasts (HFFs) host cells. HFFs were cultured in DMEM (Invitrogen) supplemented with 10% FBS (Fetal Plex Animal Serum from Gemini), 2mM L-glutamine (Gemini), and 100 ug penicillin and 100 ug streptomycin per mL (Gibco Life Technologies), maintained at 37 C and 5% CO_2. Parasites were harvested for assays by syringe lysis of infected HFF monolayers.

For transfection of *T. gondii* Δ*ku80*Δ*hxgprt*, 15ug of the pTgCRISPR plasmid was combined with 3 ug of the pFtsH1N805S or pFtsH1WT that had been linearized by NotI digestion. Approximately 10^7 parasites were released from host cells using syringe lysis and washed into 400uL of cytomix containing both plasmids. Parasites were eletroporated (BTX Electro Cell Manipulator 600) with 1.2-1.4 kV, 2.5kV/resistance, R2 (24 ohm) and then allowed to recover in the cuvette at room temperature for 10 mins before adding to host cells. After 24 hours, media containing 25ug/mL mycophenolic acid (Sigma) and 50 ug/mL xanthine (Sigma) was added to select for transfectants. After a week, plaques were observed and single clones were isolated using limiting dilution.

Toxoplasma gondii genome sequencing and SNP identification

Actinonin resistant and susceptible *T. gondii* were grown on 15 cm dishes containing confluent HFF monolayers until spontaneous lysis of the monolayer was achieved. Released parasites were collected and filtered through 5 micrometer syringe filters (Millipore) before isolating DNA (Qiagen DNAeasy Blood & Tissue).

T. gondii genomic DNA isolated from either the parental *T. gondii* RH strain (SRR3666219) or any of its derived mutants (SRR3666219, SRR3666222, SRR3666224,

SRR3666792, SRR3666794, SRR3666796, SRR3666798, SRR3666799, SRR3666801) was sequenced in an Illumina NextSeq apparatus using 2x150bp reads at an average sequencing depth of 35x. Sequencing reads were quality trimmed and remnants of sequencing adaptors removed with *trimmomatic* (PMID:24695404). Next, reads were mapped to the reference nuclear assembly of the *T. gondii* GT1 strain (ToxoDB v13.0) and the apicoplast genome assembly from the RH strain (NC_001799) with the program *bowtie2* (PMID:25621011). Duplicated aligned reads were removed with *picard tools* (**http://broadinstitute.github.io/picard**) and reads spanning InDels were realigned with GATK (PMID:20644199). Afterwards, allelic variants were called with *samtools mpileup* (PMID:19505943) followed by *bcftools call* with *–p* set to 0.05 (PMID:26826718). Finally, classification of mutations was performed with *snpEff* (PMID:22728672).

Growth inhibition assays

For *P. falciparum* EC_{50} calculations, growth assays were performed in 96 well plates containing serial dilution of drugs in triplicate. Media was supplemented with 200 uM IPP as indicated. Growth was initiated with ring-stage parasites (synchronized with 5% sorbitol treatment 48 hours prior) at 1% parasitemia and 1% hematocrit. To calculate growth, cultures were incubated for 72h and growth was then terminated by incubation with 1% formaldehyde (Electron Microscopy Services) for 30 minutes at room temperature. Parasitized cells were stained with 50 nM YOYO-1 (Invitrogen) overnight at room temperature and the parasitemia was determined by flow cytometry (BD Accuri C6 Sampler). Data were analyzed by BD Accuri C6 Sampler software.

For *T. gondii* EC_{50} calculations, plaque assays were performed in 24 well plates containing confluent HFF monolayers serial dilutions of drugs in duplicate. Approximately 50 parasites were counted using flow cytometry and added to each well. After incubating for 6 days, infected monolayers were washed, fixed with methanol for 10 minutes, stained with 2% crystal violet (Sigma) for 30 minutes, and then washed again. Plaques were visualized as non-stained areas. The area of each plaque in a given well was measured and summed using ImageJ as a proxy for growth and normalized to the vehicle only control.

For measuring the growth inhibition of *P. falciparum* during the time course, 10 uM actinonin, 10 uM fosmidomycin, 30 uM chloramphenicol, 200 uM IPP, and 0.5 uM of anhydrotetracycline was used as necessary. For comparison of growth between different treatment conditions, cultures were carried simultaneously and handled identically with respect to media changes and addition of blood cells. Daily samples were collected and fixed with 1% formaldehyde for 30 minutes at RT. At the end of the time course, all samples were stained with 50 nM YOYO-1 and parasitemia was measured using flow cytometry. All growth curves were plotted using GraphPad Prism.

For measuring the growth inhibition of *T. gondii* during the time course, 6-well plates were set up with no drug, 40 uM actinonin, 25 nM clindamycin, and 4 uM pyrimethamine. *T. gondii* was added at a MOI = 3. Every 12 hours, parasites were released from HFFs using syringe lysis and counted using flow cytometry (BD Accuri C6 Sampler). After 36 hours, spontaneous lysis of the monolayer was observed and parasites

were counted using flow cytometry and then added back to fresh monolayers at MOI = 3 in the absence of drug and parasites were counted every 12 hours as before.

For co-treatments of *P. falciparum* with actinonin and chloramphenicol, 96 well plates containing ring stage parasites at 1% parasitemia and 1% hematocrit were treated with serial dilutions of both actinonin and chloramphenicol alone and in combination. To determine the effect on growth after one lytic cycle, parasites were fixed at 72h and parasitemia was measured by flow cytometry as above. To determine the effect on growth after two lytic cycles, 75% of the media was exchanged at 72 hours and plates were incubated for an additional 48 hours following fixation and flow cytometry as above. Media was supplemented with 200 uM IPP as a separate control to insure specificity of the drug at the concentrations used.

Quantitative Real-Time PCR

Parasites from 1 mL of *P. falciparum* culture at ring stage were isolated by saponin lysis followed by two washes with PBS. DNA was purified using DNAeasy Blood & Tissue (Qiagen). Primers were designed to target genes found on the apicoplast or nuclear genome: tufA (apicoplast) 5'-GATATTGATTCAGCTCCAGAAGAAA-3' and CHT1 (nuclear) 5'-TGTTTCCTTCAACCCCTTTT-3' /5'-TGTTTCCTTCAACCCCTTTT-3'. Reactions contained template DNA, 0.15 uM of each primer, and 1x SYBR Green I Master mix (Roche). qPCR reactions were performed at 56C primer annealing and 65C template extension for 35 cycles on a Applied Biosystem 7900HT system. Relative quantification of target genes was determined[32]. For each time point, the apicoplast:nuclear genome ratio was calculated relative to the appropriate control collected at the same time.

Fluorescence Microscopy

P. falciparum D10 ACP(L)-GFP parasites diluted to 0.05% hematocrit were settled on a Lab-Tek II Chambered Coverglass (Thermo Fisher) and incubated in 2 ug/mL Hoescht 33342 stain for 15 minutes at 37C. Widefield epifluorescence live cell images were acquired with an Olympus IX70 microscope. The microscope was outfitted with a Deltavision Core system (Applied Precision) using an Olympus x60 1.4NA Plan Apo Lens, a Sedat Quad filter set (Semrock) and a CoolSnap HQ CCD Camera (Photometrics). The microscope was controlled and images were deconvolved via softWoRx 4.1.0 software. ImageJ software was used to analyze resulting images.

Live microscopy of *T. gondii* RH FNR-RFP parasites[36] was performing using Lab-Tek II Chambered Coverglasses containing confluent HFF monolayers. Parasites were added at an MOI = 1. After 36 hours of incubation, parasites were incubated with 2 ug/mL of Hoescht for 15 minutes. Widefield epifluorescence live cell images were acquired with a Nikon Eclipse Ti inverted fluorescence microscope with a NA 1.40 oil-immersion objective (Nikon Instruments) and controlled using MicroManager v1.4. An iXon3 888 EMCCD camera (Andor) was used for fluorescence imaging and an a Zyla 5.5 sCMOS camera (Andor) was used for phase contrast imaging. ImageJ software was used to analyze the resulting images.

Immunoblot

Parasites from 9 mL of *P. falciparum* culture were isolated by saponin lysis, washed with PBS and resuspended in 1 x NuPAGE LDS sample buffer (Invitrogen). Proteins were separated by electrophoresis on 4-12% Bis-Tris gel (Invitrogen) and transferred to a nitrocellulose membrane. After blocking, membranes were probed with 1:2000 monoclonal mouse anti-FLAG M2 (Sigma) and 1:10,000 IRDye 680RD goat anti-mouse IgG (LiCor Bioscience). Fluorescence antibody-bound proteins were detected with Odyssey Imager at 700 nm (LiCor Biosciences).

***Toxoplasma gondii* resistance selection**

Approximately 2 x 10^6 *T. gondii* RH parasites were added to T25s containing a confluent HFF monolayer and allowed to grow for 24 hours. To mutagenize, between 500 uM – 2 mM N-ethyl N-nitrosourea (ENU) diluted in DMSO was added to flasks and incubated for 2 hours at 37 C. Cultures were then washed twice with 10mLs of cold PBS and then released from host cells using syringe lysis. A quarter of the resulting parasites were passaged to T25s containing a fresh monolayer of HFFs. After two passages, parasites were treated with 40uM actinonin. After one passage under actinonin selection, a severe bottleneck was observed. Plaques of resistant parasites could be observed after one week of constant actinonin pressure with periodic media changes. Finally, single clones were isolated using limiting dilution.

***Plasmodium falciparum* construct generation**

The primers used for generating different fragments are listed in the Extended Data Table 3. A construct for regulating expression of FtsH1 (PF3D7_1239700) in *P. falciparum* (pFtsH1) was generated from the parental pSN054, a modified pJazz linear plasmid (Extended Data Table 3). The left homology region was amplified from parasite genomic DNA using primers SMG476 and SMG 477 and was cloned using FseI and AsisI restriction sites. FtsH1 protein coding nucleotides 2348- 2643 were recoded using gene block (IDT) to remove the PAM site. The right homology region was amplified from parasite genomic DNA using primers SMG501 and SMG502. These fragments were cloned using the I-SceI restriction site. Targeting guide RNA was generated by klenow reaction using primers SMG514 and SMG515 and was inserted using the AflII site. All sequences were ligated into the parent plasmid using Gibson assembly. Constructs for regulation FtsH3 (PF3D7_1464900) were generated similarly (SMG505 and SMG506 for the right homology region; SMG495 and SMG496 for the left homology region; SMG518 and SMG519 for the gRNA klenow reaction). While this construct could be generated, no parasites emerged after two transfections. Constructs for regulating FtsH2 (PF3D7_1119600) using primers SMG503 and SMG504 for the right homology region and SMG481 and SMG507 for the left homology region were unable to be generated because of unsuccessful PCR.

***Toxoplasma gondii* construct generation**

A construct for knocking in the $FtsH1_{N805S}$ allele into the endogenous loci of FtsH1 (pFtsHN805S) was generated from the parental pTKO2 vector. Briefly, a ~800 bp sequence upstream of the TGGT1_259260 start codon was amplified as the left

460 homology region (using primers KAJ1 and KAJ2). The $FtsH_{N805S}$ sequence was then
461 amplified from actinonin resistant cDNA (using primers KAJ3 and KAJ4). The HXGPRT
462 resistance cassette was amplified off of the pTKO2 cassette (using primers KAJ5 and
463 KAJ6). A ~800 bp sequence downstream of the TGGT1_259260 stop codon was
464 amplified as the right homology region (using primers KAJ7 and KAJ8). To insert the
465 right homology region, the pTKO2 plasmid was cut with HindIII and HpaI and the 800
466 bp sequence was inserted using infusion (Clontech). To insert the left homology region
467 and the $FtsH1_{N805S}$ allele, the pTKO2 plasmid containing the downstream homology
468 region was cut with NotI and EcoRI and the two PCR products were inserted also using
469 infusion (Clontech). The resulting colonies were tested using a diagnostic HpaI digest
470 and correct clones were subjected to Sanger sequencing of the inserts. To revert the
471 pFtsHN805S construct to pFtsHWT, we used Q5 mutagenesis (NEB) and primers KAJ9
472 and KAJ10.
473
474 To increase the transfection efficiency and specificity, CRISPR-Cas9 was used to insert a
475 double stranded break at the site of insertion (the endogenous TGGT1_259260 allele).
476 Briefly, pSAG1::Cas9-U6::sgUPRT[33] was modified to contain a guide sequence specific
477 to a FtsH1 intron using the Q5 mutagenesis kit (NEB) and primers KAJ11 and KAJ12.
478 Sanger sequencing of the guide was used to verify the resulting plasmid.
479
480 31. Sidik, S. M. *et al.* A Genome-wide CRISPR Screen in Toxoplasma Identifies
481 Essential Apicomplexan Genes. *Cell* **166,** 1423–1435.e12 (2016).
482
483 32. Pfaffl, M. W. A new mathematical model for relative quantification in real-time RT-
484 PCR. *Nucleic Acids Res.* **29,** e45 (2001).
485
486 33. Shen, B., Brown, K. M., Lee, T. D. & Sibley, L. D. Efficient gene disruption in
487 diverse strains of Toxoplasma gondii using CRISPR/CAS9. *mBio* **5,** e01114-01114
488 (2014).
489
490 34. Camps, M. *et al.* A rRNA mutation identifies the apicoplast as the target for
491 clindamycin in Toxoplasma gondii. *Mol Microbiol.* **5**, 1309-18 (2002).
492
493 35. Dahl, E.L., Rosenthal, P.J. Multiple antibiotics exert delayed effects against the
494 Plasmodium falciparum apicoplast. *Antimicrob Agents Chemother.* **51,** 3485-90
495 (2007).
496
497 36. Striepen, B. *et al.* The plastid of *Toxoplasma gondii* is divided by association with
498 the centrosomes. *J Cell Biol.* **151,** 1423-1424 (2000).
499
500 **Acknowledgements**
501 We thank Katrina Hong for assistance in drug assays and Prof. Boris Striepen for
502 providing the *T. gondii* FNR-RFP strain. This project has been funded with federal funds
503 from the NIAID, NIGMS, and Director's Fund, National Institutes of Health, Department
504 of Health and Human Services under Award Numbers 1K08AI097239 (EY),
505 1DP5OD012119 (EY), U19AI110819 (HAL), 1DP2OD007124 (JCN), P50 GM098792

(JCN), and T32GM007276 (KAJ). Funding was also provided by the Burroughs-Wellcome Fund (EY), Bill and Melinda Gates Foundation (OPP1069759; JCN), and the Stanford Bio-X SIGF William and Lynda Steere Fellowship (KAJ).

Author Information

Affiliations

Department of Biochemistry, Stanford Medical School, Stanford, California 94305
Katherine Amberg-Johnson, Ellen Yeh

Department of Pathology, Stanford Medical School, Stanford, California 94305
Ellen Yeh

Department of Microbiology & Immunology, Stanford Medical School, Stanford, California, 94305
Katherine Amberg-Johnson, Ellen Yeh

Department of Biological Engineering, Massachusetts Institute of Technology, Cambridge, Massachusetts, 02139
Suresh M. Ganesan, Jacquin C. Niles

Department of Infectious Disease, The J. Craig Venter Institute, Rockville, Maryland, 20850
Hernan A. Lorenzi

Contributions

K.A-J. and E.Y. conceived and designed experiments. K.A-J. performed the majority of the experiments. S.M.G. and J.C.N. designed and generated the FtsH1 knockdown construct. H.A.L. performed the whole-genome sequencing and variant analysis. K.A-J. and E.Y. analyzed the data and wrote the manuscript. All authors discussed and edited the manuscript.

Competing financial interests

The authors declare no competing financial interests.

Corresponding author

Correspondence to: Ellen Yeh

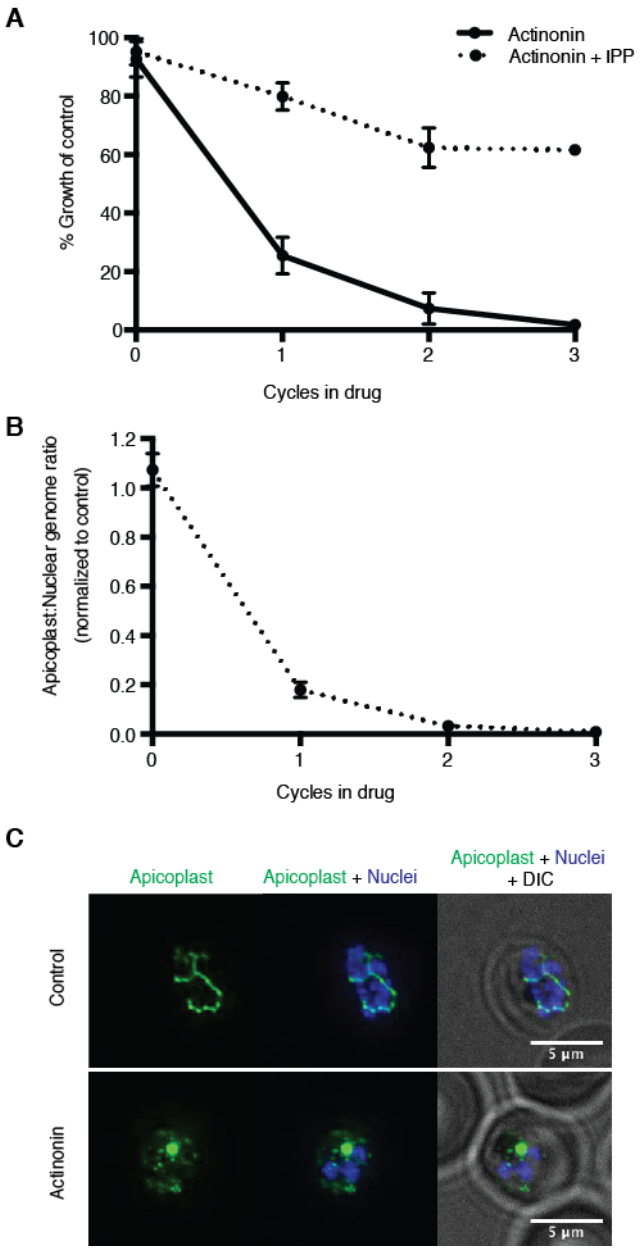

Fig 1: Actinonin inhibits apicoplast biogenesis in *P. falciparum*

(a) Time course of parasite growth during actinonin treatment with or without IPP, normalized to control cultures with or without IPP as appropriate. Error bars represent the SEM of two biological replicates.

(b) Time course of the apicoplast:nuclear genome ratio measured by quantitative PCR (qPCR) using primers for the apicoplast and nuclear genomes during treatment with actinonin and IPP. Genome ratios were normalized to control parasites grown with IPP only. Error bars as in **a.**

(c) Representative images of the apicoplast of IPP-rescued control and actinonin treated parasites 24 hours after treatment during the schizont stage. The apicoplast is visualized using the *P. falciparum* reporter strain D10 ACP-GFP in which GFP is targeted to the apicoplast and the nucleus is stained with Hoescht 33342. During *Plasmodium* replication, the apicoplast starts as a single small spherical organelle (ring stage) which branches and divides into multiple apicoplasts (schizont stage). A punctate apicoplast that does not branch indicates a defect in apicoplast biogenesis.

Fig 2: A mutation in the protease domain of *TgFtsH1* is sufficient to confer resistance to actinonin in *T. gondii*

(a) Representative images of the apicoplast of control and actinonin treated parasites 36 hours after infection. Representative parasites missing their apicoplast are denoted with white arrows. The apicoplast is visualized using the *T. gondii* reporter strain RH FNR-RFP in which RFP is targeted to the apicoplast and the nucleus is stained with Hoescht 33342. Each untreated parasite contains one apicoplast, except during cell division when there may be two.

(b) Dose-dependent parasite growth inhibition upon treatment with actinonin for the actinonin-sensitive parent strain (RH) compared with 3 independent clones following selection for actinonin resistance (resistant 1, resistant 2, resistant 3). These three resistant clones are representative of the eight clones submitted for whole genome sequencing. Growth was measured via summed areas of the plaques formed during plaque assays and normalized to untreated controls. Error bars represent the SEM of two biological replicates.

(c) Dose-dependent parasite growth inhibition upon treatment with actinonin for *TgFtsH1(WT)* compared with *TgFtsH1(N805S)* parasites in RH *ΔKU80* strain. Data was measured and analyzed as in 2b.

(d) Schematic of *Tg*FtsH1. This protein contains a *N*-unique region containing a putative transmembrane domain, an AAA ATPase domain used for unfolding proteins, a peptidase domain with a zinc co-factor in the catalytic site, and a *C*-unique region. The resistance-conferring variant *Tg*FtsH(N805S) is found in the peptidase domain near the catalytic site.

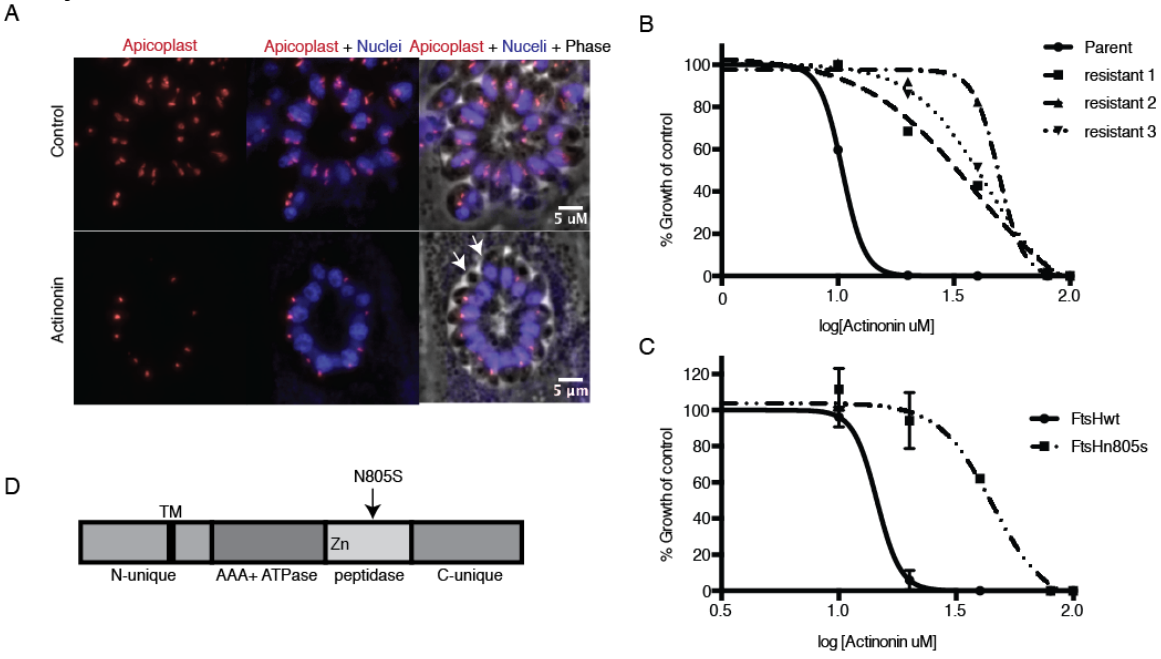

Fig 3: Knockdown of *FtsH1* in *P. falciparum* leads to apicoplast loss and hypersensitivity to actinonin
(a) Schematic of the endogenous knockdown strategy. When anhydrotetracycline (aTC) is present in the media, the tet-repressor binds aTC and does not bind the 10x-aptamer sequence, which relieves translational repression, allowing FtsH1 to be expressed. When aTC is washed out of the media, the tet-repressor binds the 10x-aptamer and prevents expression of FtsH1.
(b) Time course of parasite growth without aTC and in the presence or absence of IPP in the media, normalized to the untreated or IPP-rescued parental strain as appropriate. Error bars represent the SEM of two biological replicates.
(c) Time course of the apicoplast:nuclear genome ratio measured by quantitative PCR (qPCR) using primers for the apicoplast and nuclear genomes during treatment with or without aTC. All samples contained IPP to rescue parasite growth. Genome ratios were normalized to respective parental cultures also grown with IPP. Error bars as in **c.**
(d) Dose-dependent parasite growth inhibition by actinonin in the absence or presence of aTC. Error bars as in **c.**

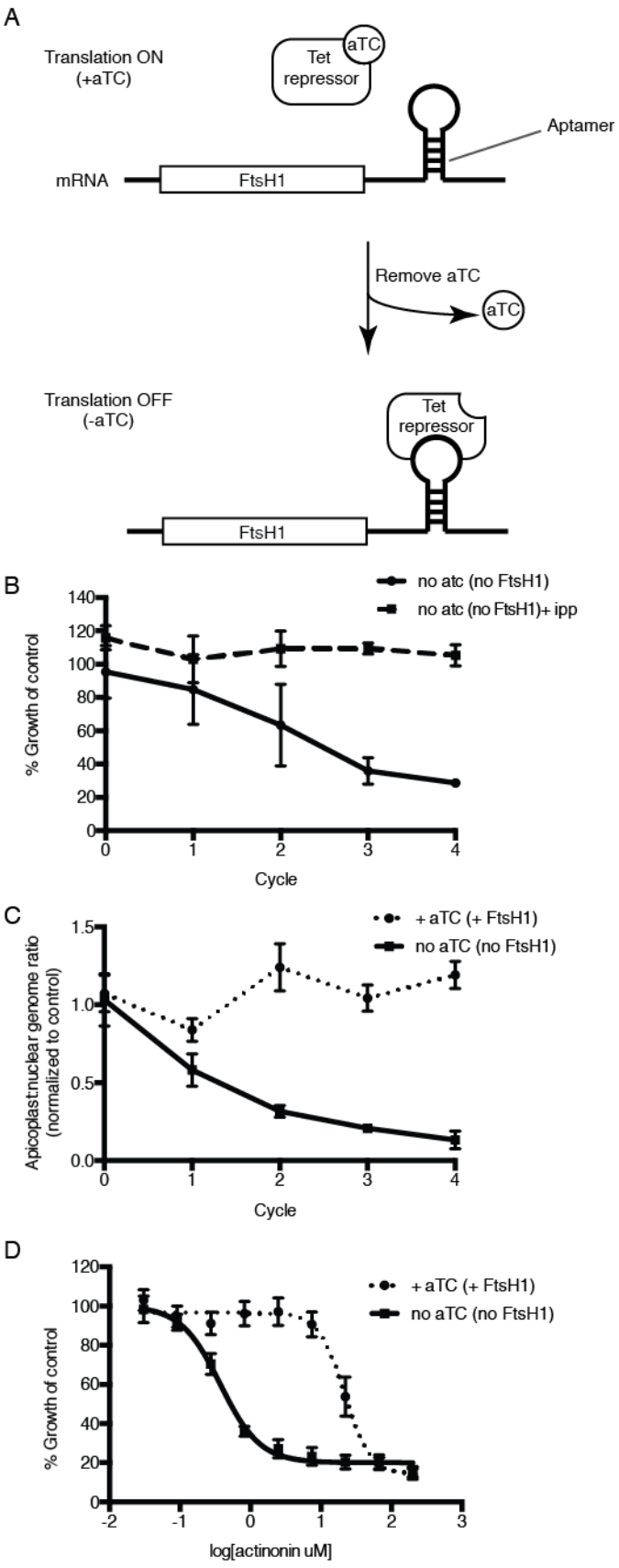

Extended Data 1: Actinonin specifically inhibits the apicoplast of *P. falciparum* leading to parasite death after a single replication cycle

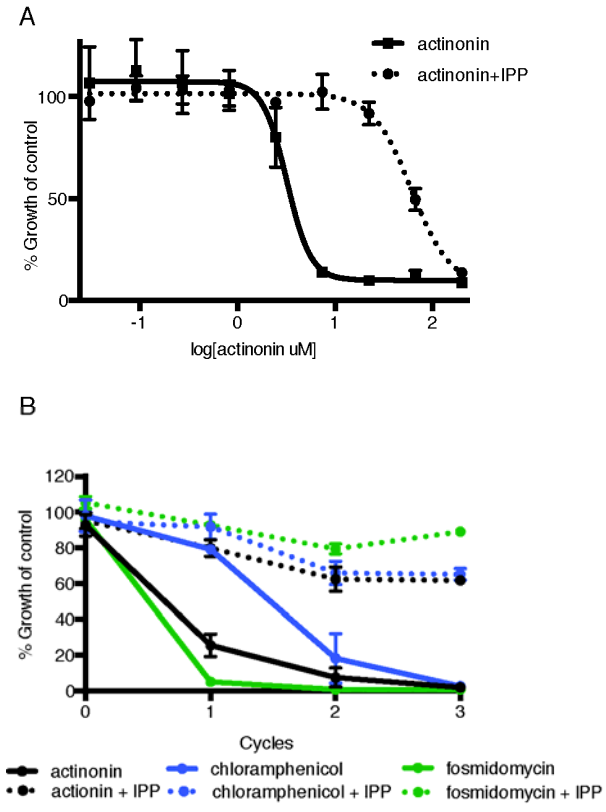

(a) Dose-dependent parasite growth inhibition by actinonin in the absence or presence of IPP. Error bars represent the standard error of the mean (SEM) of two biological replicates.

(b) Time course of parasite growth during treatment with actinonin, chloramphenicol, or fosmidomycin in the absence or presence of IPP. Growth is normalized to untreated or IPP-rescued controls as appropriate. Error bars as in **a.** In contrast to other antimalarials, which cause growth inhibition in a single replication cycle, "delayed death" in *P. falciparum* is associated with inhibitors of apicoplast gene expression and has previously been described in detail[35]. It is characterized by a normal apicoplast and cell division during drug treatment for one replication cycle, followed by halted apicoplast and cell division in daughter parasites of drug-treated parasites.

Extended Data Fig 2: Actinonin has a distinct inhibition phenotype compared to inhibitors of apicoplast metabolism and translation

(a) Time course of the apicoplast:nuclear genome ratio measured by quantitative PCR (qPCR) for targets in the apicoplast and nuclear genome during treatment with actinonin (black), chloramphenicol (blue), or fosmidomycin (green). While actinonin treatment blocks apicoplast genome replication in a single replication cycle, this effect is not observed until the second replication cycle of chloramphenicol treatment and not at all during fosmidomycin treatment. This is consistent with actinonin blocking apicoplast biogenesis, chloramphenicol blocking apicoplast translation leading to a delayed apicoplast biogenesis defect, and fosmidomycin blocking apicoplast metabolic function but not biogenesis. All samples were grown in IPP and genome ratios were normalized to the untreated control cultures also containing IPP. Error bars represent the SEM of at least 2 biological replicates.

(b-e) Representative images of the apicoplast during schizont stage of three successive replication cycles in untreated **(b),** chloramphenicol **(c)**, fosmidomycin **(d)** and actinonin **(e)** treated cultures all grown with IPP. The apicoplast is visualized using the *P. falciparum* reporter strain D10 ACP-GFP in which GFP is targeted to the apicoplast and the nucleus is stained with Hoescht 33342. In this case, a branched apicoplast indicates successful apicoplast development while punctate apicoplasts (observed in replication cycle 1 for actinonin treatment (e) and replication cycle 2 for chloramphenicol treatment (c)) represents an apicoplast that has failed to develop. The apicoplast is no longer present after replication cycle 2 of actinonin treatment and upon replication cycle 3 of chloramphenicol treatment, which leads to complete mislocalization of the GFP.

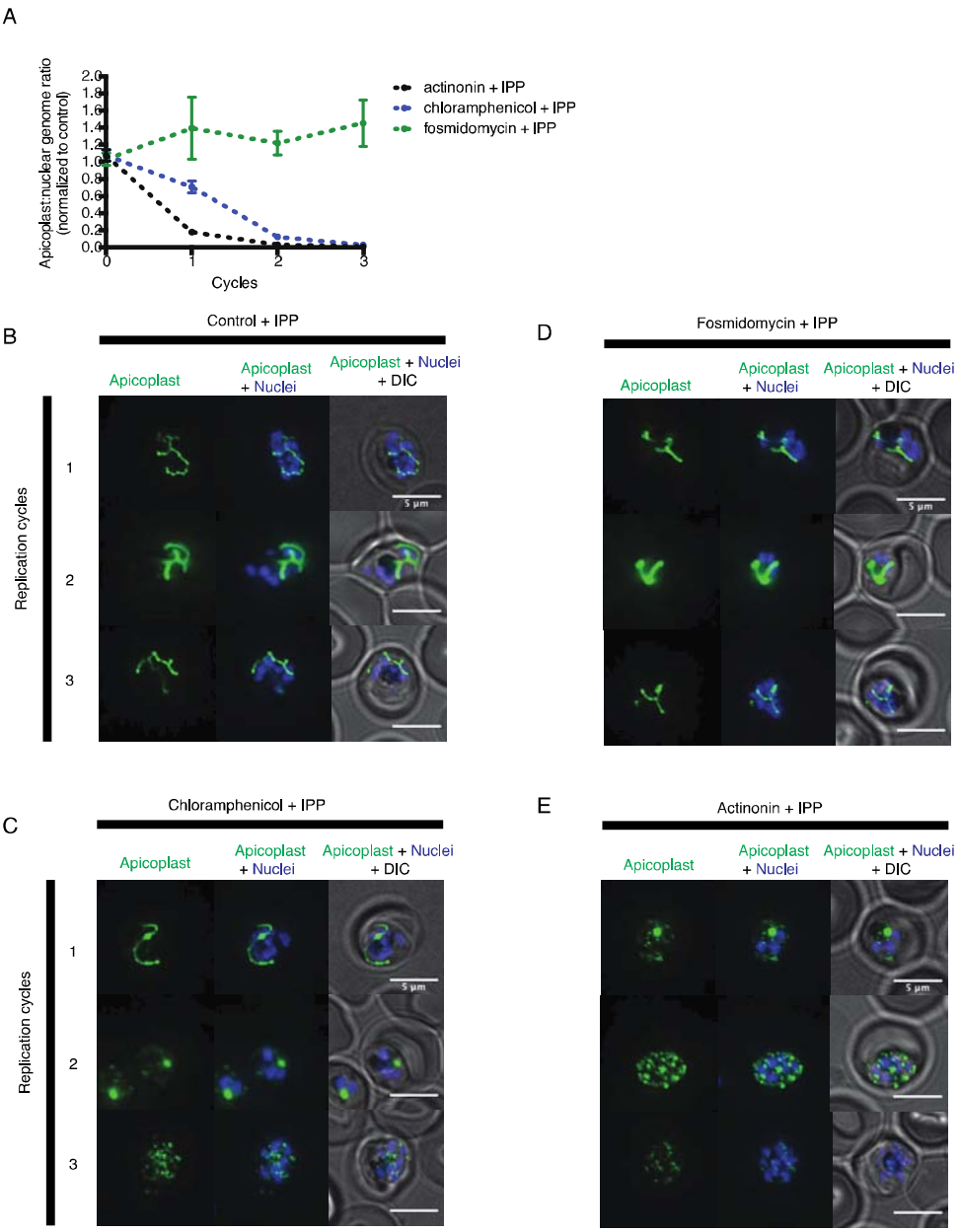

694

Extended Data Fig 3: Growth inhibition in the first replication cycle by actinonin is not suppressed by apicoplast translation inhibition

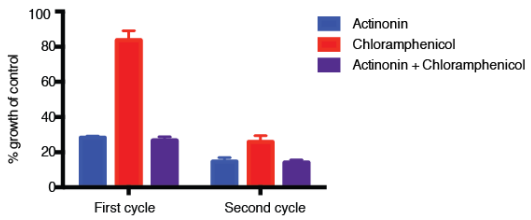

Parasite growth after one or two replication cycles after treatment with actinonin, chloramphenicol, or both actinonin and chloramphenicol normalized to growth of an untreated control. Treatment with actinonin alone inhibited growth after the first replication cycle, whereas treatment with chloramphenicol alone inhibited growth after the second replication cycle. Co-treatment with chloramphenicol, which targets apicoplast translation, did not suppress effects of actinonin treatment, which was inconsistent with actinonin targeting the peptide deformylase (PDF) of the apicoplast.

Extended Data Fig 4: Actinonin treatment causes "delayed death" in *T. gondii* associated with apicoplast loss

Time course of parasite growth of untreated (blue), clindamycin (green), pyrimethamine (black), or actinonin (red) treated parasites over the course of two lytic cycles. Unlike *P. falciparum*, *T. gondii* undergoes multiple replication cycles in the host cell before lysis, thus each *T. gondii* lytic cycle represents multiple parasite replication cycles. Pyrimethamine inhibits parasite dihydrofolate reductase and was used as a control for a non-apicoplast targeting drug that inhibits growth in a single lytic cycle. As previously reported[34], clindamycin, an apicoplast translation inhibitor, gave a "delayed death" phenotype in *T. gondii* characterized by completed cell divisions and host re-invasion during drug treatment in the first lytic cycle, followed by halted cell division in the second lytic cycle. Actinonin also led to growth inhibition in the second lytic cycle, suggesting that it also targets the apicoplast. Error bars represent the SEM of two biological replicates. It is important to distinguish between apicoplast-associated "delayed death" in *P. falciparum* and that in *T. gondii*. In *T. gondii*, apicoplast loss occurs in the first lytic cycle and is temporally separate from defects in parasite cell division and growth inhibition observed in the second lytic cycle; whereas in *P. falciparum* defects in apicoplast biogenesis, parasite cell division, and growth inhibition all occur in the second replication cycle. "Delayed death" in *T. gondii* therefore appears more broadly associated with disruption of apicoplast biogenesis, where "delayed death" in *P. falciparum* appears more specific to disruption of apicoplast gene expression that leads to delayed biogenesis defects.

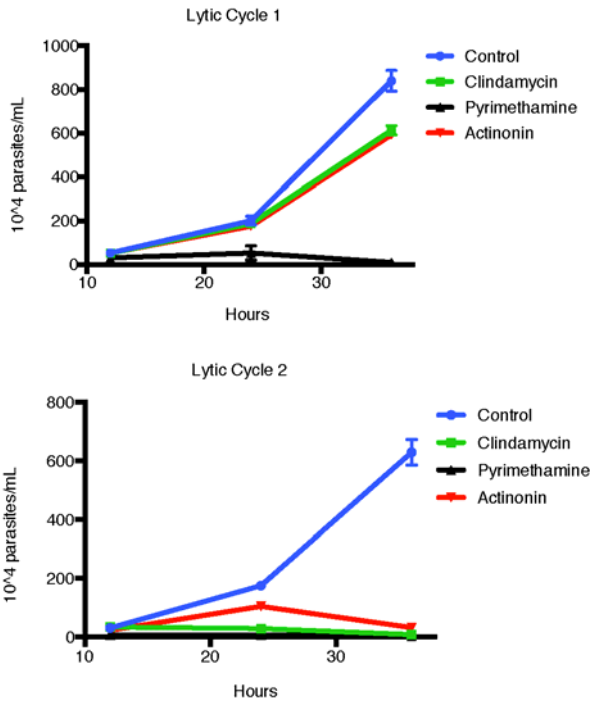

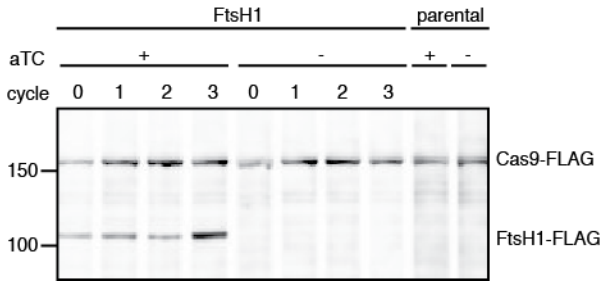

Extended Data Fig 5: Removal of anhydrotetracycline (aTC) from the media results in efficient knockdown of *Pf*FtsH1.

Consistent with the previous report of *Pf*FtsH1 *C*-terminal processing, we were unable to detect full-length *Pf*FtsH1-FLAG using anti-FLAG in parasites with intact apicoplasts. However, upon loss of the apicoplast, full-length *Pf*FtsH1-FLAG was detectable, suggesting that *Pf*FtsH1 processing occurs in the apicoplast. Therefore, to assess the knockdown efficiency of *Pf*FtsH1, we used a western blot comparing *Pf*FtsH1-FLAG levels in the presence (lanes 1-4) or absence of aTC (lanes 5-8) in IPP-rescued parasites missing their apicoplast. Each sample was taken at the trophozoite stage and cycle 0 indicates 24 hours after the removal of aTC. Lanes 9 and 10 are samples from the parental strain that do not contain the FLAG-tag or the aptamer sequence in the 3' UTR of *Pf*FtsH1. In each case, Cas9-FLAG was used as a loading control. *Pf*FtsH1-FLAG levels were reduced to undetectable levels at 24 hours after aTC removal, validating our knockdown strategy.

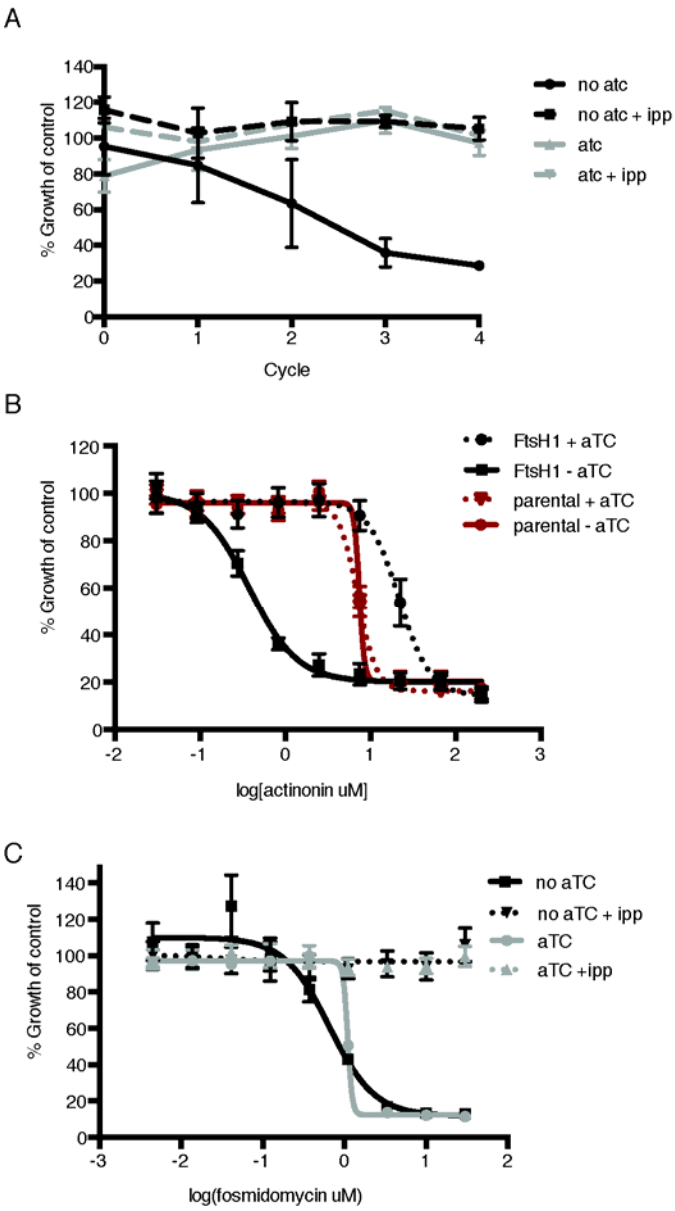

Extended Data Fig 6: Knockdown of *Pf*FtsH1 specifically disrupts the apicoplast and leads to specific hypersensitivity to actinonin

(a) Time course of parasite growth with or without anhydrotetracycline (aTC) and with or without IPP in the media. IPP rescues the growth defect observed in upon *Pf*FtsH1 downregulation, indicating that *Pf*FtsH1 is essential for an apicoplast-specific function. Growth is shown normalized to the untreated or IPP-rescued parental strain as appropriate. Error bars represent the SEM of two biological replicates.

(b) Dose-dependent parasite growth inhibition by actinonin with or without aTC for the parental (red) and *Pf*FtsH (black) strain. The EC_{50} of the parental strain is unchanged by the removal of aTC. Error bars as in **a.**

(c) Dose-dependent parasite growth inhibition by fosmidomycin with or without aTC in and with or without IPP. The fosmidomycin EC_{50} is unchanged by regulating levels of *Pf*FtsH1, indicating that the observed hypersensitivity to actinonin upon knockdown of *Pf*FtsH1 is specific to actinonin and does not occur for all apicoplast drug. Error bars represent the SEM of three technical replicates.

797